

A Proportional-Integral Controller for Distance-Based Formation Tracking

Oshri Rozenheck¹, Shiyu Zhao², and Daniel Zelazo²

Abstract—This work considers a multi-agent formation control problem where a designated leader is subjected to an additional velocity reference command. The entire formation should follow the leader while maintaining the inter-agent distance constraints. By augmenting a standard gradient formation controller with a proportional-integral control on the formation error, we are able to prove the stability of the formation error dynamics with velocity input while ensuring zero steady-state formation error. Numerical simulations are shown to illustrate the theoretical results.

I. INTRODUCTION

In recent years, there has been much attention given to the control of formations of multiple agents across many application domains. Of the many control strategies for formation control, distance-constrained formation stabilization has been extensively studied [1]–[8]. A closely related problem is formation tracking where the objective is to find a control scheme that allow multiple robots to maintain some given formation while executing additional tasks such as velocity tracking or leader following.

Distance-constrained formation control aims at maintaining inter-agent distances and utilizes relative measurements (i.e., distances and relative-positions) to generate the control action. The theory of rigidity has emerged as the correct mathematical foundation for defining distance-constrained formations and proving that distance-constrained formation control strategies are stabilizing [3], [9], [10].

The stability analysis of these control strategies has been investigated in many works. In [11], application of the center manifold theorem was used to prove the local stability of infinitesimally rigid formations. Lyapunov-based approaches were employed in [6], [12]. As a first contribution of our work, we provide an alternative local stability proof by deriving the dynamics of the formation error and employing Lyapunov’s indirect method.

¹O. Rozenheck is with the Technion Autonomous Systems Program, Technion - Israel Institute of Technology, Haifa, Israel. oshriroz@tx.technion.ac.il

²S. Zhao, and D. Zelazo are with the Faculty of Aerospace Engineering, Technion - Israel Institute of Technology, Haifa, Israel. szhao@tx.technion.ac.il, dzelazo@technion.ac.il

Despite its apparent utility, there are very few existing studies addressing velocity tracking in formation control. The aid of one or more virtual agents to help the formation achieve a desired common velocity or to arrive at a desired destination is considered in [13], [14]. In particular, [15] proposed a flocking algorithm with a virtual leader by including a navigational feedback mechanism to every agent under the assumption that all agents are being informed. In [6], [14], [16], the formation tracking problem is considered for agents with second-order dynamics.

In this work, we consider a collection of agents with integrator dynamics tasked with maintaining a distance-constrained formation. One agent in the ensemble is also designated as a leader and is subjected to an external velocity reference command. In the absence of any additional control action, the standard rigidity based formation stabilization solutions will exhibit a steady-state formation error [17]. To address this, we augment the gradient based formation controller with a proportional and integral (PI) control on the formation error. We show that such a scheme preserves the stability properties of the formation error dynamics while ensuring a zero steady-state formation error. This scheme has many advantages, including a simple and distributed implementation and no need for virtual leaders.

The paper is organized as follows. An overview on rigidity theory is provided in Section II. The well known distance-constrained formation control law and stability analysis is presented in Section III. The PI formation controller with stability and performance analysis is presented in Section IV. Numerical simulations are given in Section V to verify the theoretical results. Section VI contains concluding remarks and areas for future work.

Notations: Given $A_1, \dots, A_n \in \mathbb{R}^{p \times q}$, when the range of i is clear from the context, denote $\text{diag}(A_i) \triangleq \text{blkdiag}\{A_1, \dots, A_n\} \in \mathbb{R}^{np \times nq}$. Denote I_n as the $n \times n$ identity matrix. Let $\mathbf{1}_n = [1, \dots, 1]^T \in \mathbb{R}^n$ be the vectors of all ones. The eigenvalues of a symmetric positive semi-definite matrix A are denoted as $0 \leq \lambda_1(A) \leq \lambda_2(A) \leq \dots \leq \lambda_n(A)$.



II. PRELIMINARIES

A. Graph Theory

An *undirected graph* $\mathcal{G} = (\mathcal{V}, \mathcal{E})$ consists of a vertex set \mathcal{V} and an edge set $\mathcal{E} \subseteq \mathcal{V} \times \mathcal{V}$, where an edge (i, j) is an unordered pair of distinct nodes i and j . We denote the number of nodes in a graph as $n \triangleq |\mathcal{V}|$ and the number of edges as $m \triangleq |\mathcal{E}|$. If $(i, j) \in \mathcal{E}$, then i and j are said to be *adjacent*. The set of neighbors of vertex i is denoted as $\mathcal{N}_i \triangleq \{j \in \mathcal{V} : (i, j) \in \mathcal{E}\}$, and also noted as $i \sim j$. An *orientation* of an undirected graph is the assignment of a direction to each edge. An *oriented graph* is an undirected graph together with a particular orientation. The *incidence matrix* $E \in \mathbb{R}^{n \times m}$ of an oriented graph is the $\{0, \pm 1\}$ matrix with rows indexed by vertices and columns by edges. For any connected graph, it then follows that $\text{Null}(E^T) = \text{span}\{\mathbf{1}_n\}$ [18]. The *Laplacian* of a graph is a symmetric matrix defined as $L(\mathcal{G}) = EE^T$.

B. Rigidity Theory

Rigidity theory plays an important role in distance-based formation control. We next review some important definitions and results from rigidity theory; for a more detailed review, see [3], [9].

A d -dimensional *configuration* is a finite collection of n points, $x = [x_1^T, \dots, x_n^T]^T \in \mathbb{R}^{2n}$, where $x_i \in \mathbb{R}^2$ and $x_i \neq x_j$ for all $i \neq j$. A *framework*, denoted as $\mathcal{G}(x)$, is an undirected graph \mathcal{G} together with a configuration x , where vertex i in the graph is mapped to the point x_i . It is often useful to work with oriented graphs. Suppose $(i, j) \in \mathcal{E}$ corresponds to the k th directed edge in an oriented graph and define the edge vectors for a framework, sometimes called the relative position vector, as $e_k \triangleq x_j - x_i$. The edge vectors of the entire framework can be denoted as $e = [e_1^T \dots e_m^T]^T \in \mathbb{R}^{2m}$.

Two frameworks $\mathcal{G}(x)$ and $\mathcal{G}(y)$ in \mathbb{R}^2 are *equivalent* if $\|x_i - x_j\| = \|y_i - y_j\|$ for all $\{(i, j)\} \in \mathcal{E}$. Two frameworks $\mathcal{G}(x)$ and $\mathcal{G}(y)$ in \mathbb{R}^2 are *congruent* if $\|x_i - x_j\| = \|y_i - y_j\|$ for all $i, j \in \mathcal{V}$. A framework $\mathcal{G}(x)$ is *globally rigid* if every framework that is equivalent to $\mathcal{G}(x)$ is also congruent to $\mathcal{G}(x)$. A framework $\mathcal{G}(x)$ is *rigid* if there exists an $\epsilon > 0$ such that if framework $\mathcal{G}(y)$ is equivalent to $\mathcal{G}(x)$ and satisfies $\|y_i - x_i\| \leq \epsilon$ for all $i \in \mathcal{V}$, then $\mathcal{G}(y)$ is congruent to $\mathcal{G}(x)$.

Given an arbitrary oriented graph, consider a framework $\mathcal{G}(x)$ with the edge vectors as $\{e_k\}_{k=1}^m$. Define the *edge function*, $F : \mathbb{R}^{2n} \times \mathcal{G} \rightarrow \mathbb{R}^m$ as

$$F(x, \mathcal{G}) \triangleq [\|e_1\|^2, \dots, \|e_m\|^2]^T.$$

The *rigidity matrix* $R(x)$ associated with a framework $\mathcal{G}(x)$ is the Jacobian of the edge function, $R(x) \triangleq$

$\partial F(x, \mathcal{G}) / \partial x \in \mathbb{R}^{m \times 2n}$. A short calculation shows that $R(x)$ can be equivalently written as

$$R(x) = \text{diag}(e_i^T)(E^T \otimes I_2). \quad (1)$$

The *symmetric rigidity matrix* associated with a framework $\mathcal{G}(x)$ is the $2n \times 2n$ matrix defined as $\mathcal{R}(x) \triangleq R(x)^T R(x)$ [2].

If dx satisfies $R(x)dx = 0$, then dx is called an *infinitesimal flex* of $\mathcal{G}(x)$. Framework $\mathcal{G}(x)$ is *infinitesimally rigid* if the only infinitesimal flexes are trivial, i.e., are the rigid body rotations and translations of the framework. A framework $\mathcal{G}(x)$ is *minimally infinitesimally rigid* (MIR) if it is infinitesimally rigid and the number of edges is $m = 2n - 3$.

Lemma 1. ([19]) *A framework $\mathcal{G}(x)$ is infinitesimally rigid if and only if $\text{rank}(R(x)) = 2n - 3$.*

Since there are $2n - 3$ edges in an MIR framework, the number of rows of the rigidity matrix must also be $2n - 3$, leading to the following corollary.

Corollary 1. *If a framework is MIR, then the rigidity matrix $R(x)$ has full row rank.*

Corollary 1 gives a sufficient condition for the rigidity matrix of a framework having full row rank. The notion of MIR frameworks and Corollary 1 turn out to be an important property for deriving the stability of distance-constrained formation problems [20].

III. DISTANCE-CONSTRAINED FORMATION STABILIZATION

In this section, we first present the well known gradient control law for distance-constrained formation problems [11]. A contribution of this section is to derive an associated dynamical system based on the formation error. We then provide an alternative stability proof using the error dynamics and Lyapunov's indirect method.

Consider n ($n \geq 2$) agents, modeled as kinematic point masses, moving in a 2-dimensional Euclidean space. The motion of the agents are modeled as first-order integrators,

$$\dot{x}_i(t) = u_i(t), \quad i = 1, \dots, n, \quad (2)$$

where $x_i(t) \in \mathbb{R}^2$ is the position of the i -th robot and $u_i(t) \in \mathbb{R}^2$ denotes the control input.

Denote $d \in \mathbb{R}^m$ as the *distance constraint vector* with d_k as its entries. Each entry, d_k , represents the desired distance between agent i and j for edge $(i, j) \in \mathcal{E}$.

The *distance error* $\delta \in \mathbb{R}^m$ is defined as the difference between the measured relative distances and the desired inter-agent distances,

$$\delta_k = \|e_k\|^2 - d_k^2, \quad k \in \{1, \dots, m\}. \quad (3)$$

In [11], a gradient control law was proposed to locally and asymptotically stabilize infinitesimally rigid formations. The associated positive semi-definite potential function is defined as

$$\Phi(e) = \frac{1}{2} \sum_{k=1}^m \left(\|e_k\|^2 - d_k^2 \right)^2 = \frac{1}{2} \sum_{k=1}^m \delta_k^2. \quad (4)$$

Observe that $\Phi(e) = 0$ if and only if $\|e_k\|^2 = d_k^2 \forall k = 1, \dots, m$. The control for each agent is then taken as the negative gradient of the potential function (4),

$$u_i(t) = - \left(\frac{\partial \Phi(e)}{\partial x_i} \right) = - \sum_{j \sim i} \left(\|e_k\|^2 - d_k^2 \right) e_k. \quad (5)$$

The closed loop dynamics can be written in state-space form as

$$\dot{x}(t) = -\mathcal{R}(x)x(t) + R(x)^T d. \quad (6)$$

A. Distance Error Dynamics and Stability Analysis

We now provide an alternative approach for the local stability analysis of the distance-constrained formation control in (6). Factorization of the dynamics in (6) yields

$$\dot{x}(t) = -R(x)^T (R(x)x(t) - d). \quad (7)$$

Note that from (1) it can be seen that the expression $R(x)x(t) - d$ is precisely the distance error defined in (3), i.e.,

$$\delta \triangleq R(x)x(t) - d = \text{diag}(e_i^T) \underbrace{(E^T \otimes I_2)x(t)}_e - d. \quad (8)$$

As we are concerned with the behavior of the formation error, we now derive the formation error dynamics by differentiating (8) with respect to time,

$$\dot{\delta} = 2 \text{diag}(e_i^T) \dot{e} = 2 \text{diag}(e_i^T) (E^T \otimes I_2) \dot{x}. \quad (9)$$

Combining (1) and (7) yields

$$\dot{\delta} = f(\delta) = -2R(x)R(x)^T \underbrace{(R(x)x(t) - d)}_{\delta}. \quad (10)$$

It is well known that the direct linearization of (6) around the target formation has multiple eigenvalues at the origin, and consequently cannot be analyzed by Lyapunov's indirect method [11]. In contrast, we now show that the linearization of the δ -dynamics in (10) leads to a Hurwitz state matrix, and thus local asymptotic stability is readily shown. In this direction, we first

introduce the following assumption, which is widely used in the literature [8], [12].

Assumption 1. A framework $\mathcal{G}(x)$ satisfying the distance constraints $\{d_{ij}\}_{(i,j) \in \mathcal{E}}$ is minimally infinitesimally rigid.

Theorem 1. Under Assumption 1, the origin of the formation error dynamics (10) is locally asymptotically stable.

Proof. Define a set $\Omega = \{x | R(x)x - d = 0\}$. For any $x^* \in \Omega$, $\delta = 0$ by definition, hence any $x^* \in \Omega$ corresponds to an equilibrium of (10). Denote $M(x) = R(x)R(x)^T$. Evaluating the Jacobian of the dynamics (10) at the equilibrium $\delta = 0$ ($x = x^*$) gives

$$\begin{aligned} \left. \frac{\partial f(\delta)}{\partial \delta} \right|_{\delta=0, x=x^*} &= \left. \frac{\partial (-2M(x)\delta)}{\partial \delta} \right|_{\delta=0, x=x^*} \\ &= -2 \left(\left. \frac{\partial (M(x))}{\partial \delta} \delta \right|_{\delta=0, x=x^*} - 2 \left(M(x) \frac{\partial \delta}{\partial \delta} \right) \right) \Big|_{\delta=0, x=x^*}. \end{aligned} \quad (11)$$

The linearized dynamics can thus be expressed as

$$\dot{\tilde{\delta}} = -2M(x^*)\tilde{\delta}, \quad (12)$$

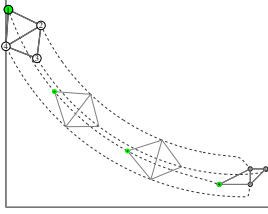
where $\tilde{\delta}$ is the variation of the state around the equilibrium point.

From Assumption 1 and Corollary 1, it follows that $R(x^*)$ has full row rank, and therefore $M(x^*)$ is a symmetric positive-definite matrix. Thus, the equilibrium point $\delta = 0$ of the nonlinear formation error dynamics is locally asymptotically stable. \square

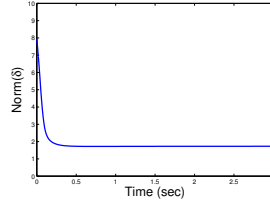
The result of Theorem 1 shows that examining the linearized formation error dynamics allows for the use of Lyapunov's indirect method to show local asymptotic stabilization of the formation. In fact, exponential stability can also be shown using a similar approach as found in [12].

IV. FORMATION CONTROL WITH VELOCITY REFERENCE

We now consider the formation controller in (6) and designate one agent as a leader. The leader is injected with an external reference velocity command, and the objective of the formation is to follow the leader while maintaining the formation shape. Without the presence of any additional control, such a scheme will always lead to a steady-state error for the formation (i.e., $\lim_{t \rightarrow \infty} \|\delta(t)\| > 0$) [17]. This phenomena is demonstrated by a simple example shown in Figure 1(a). Here, 4 agents are tasked with maintaining a diamond shape formation (satisfying Assumption 1) while tracking the



(a) An MIR formation tracking a leader.



(b) A plot of $\|\delta(t)\|$ showing a steady-state error.

Fig. 1: Without any additional control, tracking a leader leads to a steady-state error in the formation.

designated leader (marked in green). Figure 1(b) plots $\|\delta(t)\|$ showing a non-zero steady-state error.

The addition of a velocity reference to the agent designated as a leader together with the control law in (5) leads to the following dynamics,

$$\dot{x}(t) = -R(x)^T(R(x)x(t) - d) + Bv_{ref}. \quad (13)$$

Here, $B \in \mathbb{R}^{2n \times 2}$ is used to indicate which agent in the formation may receive the external velocity reference, $v_{ref} \in \mathbb{R}^2$ (i.e., if agent i is the leader, then the i th block of B is I_2 , and the remaining blocks are zero). The dynamics of the formation error vector with an external velocity reference can be derived from (13) as

$$\dot{\delta} = -2R(x)R(x)^T \kappa_P \delta + 2R(x)Bv_{ref}. \quad (14)$$

The steady-state error in the formation can be eliminated by introducing an appropriate stabilizing control into the control loop. A general control scheme is presented in Figure 2 and can be described as

$$\dot{x}(t) = u(t) + Bv_{ref}, \quad (15)$$

$$u(t) = -R(x)^T C(R(x)x(t) - d), \quad (16)$$

where $C(R(x)x(t) - d) = C(\delta)$, can be any stabilizing controller. In addition to preserving the stability of the closed-loop dynamics, the controller C should also eliminate the steady-state formation error dynamics, i.e.,

$$\lim_{t \rightarrow \infty} \|\delta(t)\| = 0.$$

Before analyzing the stability of the control scheme proposed in (16), we first examine the performance of the formation with a leader. In particular, we show that for the dynamics in (16), assuming that C is a stabilizing controller, the velocity of the formation centroid will move at a velocity proportional to the reference, v_{ref} .

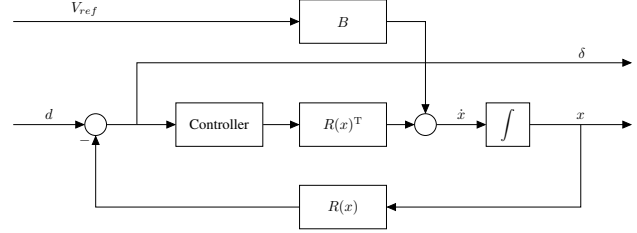


Fig. 2: The formation control is augmented with an additional controller to eliminate the steady-state error in the formation.

In this direction, first define the centroid as

$$\bar{x}(t) = \frac{1}{n} \sum_{i=1}^n x_i(t) = \frac{1}{n} (\mathbf{1}_n^T \otimes I_2) x(t). \quad (17)$$

Theorem 2. Consider the system (15) and (16) and assume C is a stabilizing controller. Then the centroid of the formation, (17), moves at the constant velocity v_{ref}/n .

Proof. Observe from (1) that $(\mathbf{1}_n^T \otimes I_2) R(x)^T = (\mathbf{1}_n^T \otimes I_2) (E \otimes I_2) \text{diag}(e_i) = 0$ due to the fact that $\mathbf{1}_n$ is the left null space of E . Using this property, we examine the dynamics of the centroid,

$$\begin{aligned} \dot{\bar{x}} &= \frac{1}{n} (\mathbf{1}_n^T \otimes I_2) (-R(x)^T C(\delta) + Bv_{ref}) \\ &= \frac{1}{n} (\mathbf{1}_n^T \otimes I_2) Bv_{ref}. \end{aligned}$$

In the case that only one agent is being controlled (i.e., $(\mathbf{1}_n^T \otimes I_2)B = I_2$), the centroid dynamics reduce to $\dot{\bar{x}} = v_{ref}/n$, concluding the proof. \square

Remark 1. Note that the centroid does not actually track the reference velocity. However, if the number of agents in the ensemble is known by the leader, this is easily overcome by premultiplication of the reference velocity by the number of agents in the network.

A *proportional controller* is a control loop feedback mechanism widely used in industrial control systems, and it is the first intuitive control gain that comes to mind when implementing a controller. The P controller is examined thoroughly in [17] and we summarize below the main result.

Theorem 3 ([17]). In the local sense, under Assumption 1, the error dynamics (14) is bounded input bounded output (BIBO) stable. Furthermore, for a constant reference velocity v , the steady-state error, δ_{ss} , can be bounded as

$$\|\delta_{ss}\| \leq \frac{\sqrt{d_{max} \cdot \lambda_n(L(\mathcal{G}))}}{\lambda_1(M(x^*))} \|v\|,$$

where d_{max} is the largest entry of vector d defined in Section III.

We now propose a proportional-integrator (PI) control for the formation error controller C aimed at eliminating the steady-state formation error when tracking a constant velocity.

A. Proportional-Integral Control

A proportional controller generally operates with a steady-state error, sometimes referred to as droop. Droop may be mitigated by adding a compensating bias term to the set point or output, or corrected dynamically by adding an integral term. The next equation describes a proportional-integrator controller that may be implemented as the controller C in (16),

$$u(t) = -R(x)^T \kappa_P (R(x)x(t) - d) - R(x)^T \kappa_I \int_0^T (R(x)x(\tau) - d) d\tau, \quad (18)$$

where κ_P and κ_I are scalar constants.

The integrator used in the controller introduces a new state-variable into the system,

$$\dot{\zeta} = \kappa_I (R(x)x(t) - d), \quad (19)$$

and by combining (15) with control law (18) the closed-loop dynamics can be expressed as

$$\begin{bmatrix} \dot{x}(t) \\ \dot{\zeta}(t) \end{bmatrix} = \begin{bmatrix} -\kappa_P R(x)^T R(x) & -R(x)^T \\ \kappa_I R(x) & 0 \end{bmatrix} \begin{bmatrix} x(t) \\ \zeta(t) \end{bmatrix} + \begin{bmatrix} \kappa_P R(x)^T \\ -\kappa_I I \end{bmatrix} d + \begin{bmatrix} B \\ 0 \end{bmatrix} v_{ref}. \quad (20)$$

Examining the system from the error vector point of view will be helpful when discussing the stability near the origin. By a coordinate transformation as in (9), and by using (20), the formation error dynamics are

$$\begin{bmatrix} \dot{\delta}(t) \\ \dot{\zeta}(t) \end{bmatrix} = \begin{bmatrix} -2\kappa_P M(x) & -2M(x) \\ \kappa_I I & 0 \end{bmatrix} \begin{bmatrix} \delta(t) \\ \zeta(t) \end{bmatrix} + \begin{bmatrix} -2R(x)B \\ 0 \end{bmatrix} v_{ref}, \quad (21)$$

where $M(x) = R(x)R(x)^T$.

Theorem 4. *Given that Assumption 1 holds, for any $\kappa_P, \kappa_I > 0$, the origin of the zero-input ($v_{ref} = 0$) error-dynamics in (21) is asymptotically stable.*

Proof. By following a similar procedure as in Theorem 1, we note that for any $x^* \in \Omega$, δ is zero by definition, which in turn leads to the equilibrium condition $\zeta = 0$.

Hence, any $x^* \in \Omega$ corresponds to an equilibrium point. Denote

$$A(x) = \begin{bmatrix} -2\kappa_P R(x)R(x)^T & -2R(x)R(x)^T \\ \kappa_I I & 0 \end{bmatrix}.$$

Linearizing around $x = x^*$ gives us the linearized dynamics

$$\begin{bmatrix} \dot{\tilde{\delta}}(t) \\ \dot{\tilde{\zeta}}(t) \end{bmatrix} = \begin{bmatrix} -2\kappa_P M(x^*) & -2M(x^*) \\ \kappa_I I & 0 \end{bmatrix} \begin{bmatrix} \tilde{\delta}(t) \\ \tilde{\zeta}(t) \end{bmatrix},$$

where $M(x^*) = R(x^*)R(x^*)^T$ as before.

By Assumption 1, $M(x^*)$ is a symmetric positive-definite matrix, and therefore all of its eigenvalues are real and positive. Denote the eigenvalues of $M(x^*)$ as μ_i . In order to learn about the location of the eigenvalues of $A(x^*)$, we need to solve its characteristic equation. The following lemma will be useful for the analysis.

Lemma 2. ([21]) *The determinant of a block matrix*

$A = \begin{bmatrix} A_{11} & A_{12} \\ A_{21} & A_{22} \end{bmatrix}$ *is given by the formula*

$$|A| = |A_{22}| |A_{11} - A_{12}A_{22}^{-1}A_{21}|. \quad (22)$$

From Lemma 2, the characteristic polynomial of $A(x^*)$ is thus

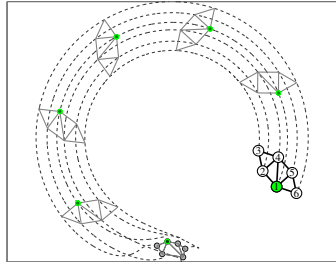
$$\begin{aligned} |\lambda I - A(x^*)| &= |\lambda^2 I + (2\kappa_P \lambda + 2\kappa_I) M(x^*)| \\ &= \prod_{i=1}^m (\lambda^2 + (2\kappa_P \lambda + 2\kappa_I) \mu_i). \end{aligned}$$

where the second equality can be derived by using the fact that $M(x^*)$ is symmetric and thus also diagonalizable. The i th eigenvalue of $A(x)$ can be computed as

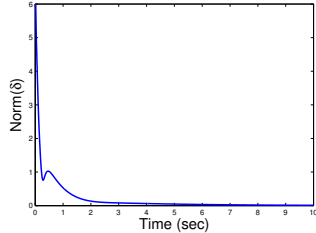
$$\lambda_i = \frac{-2\kappa_P \mu_i \pm \sqrt{4(\kappa_P \mu_i)^2 - 8\kappa_I \mu_i}}{2}. \quad (23)$$

Since $\mu_i > 0$ is positive, it follows that κ_P must be positive in order for the real part of λ_i to be in the open left-half plane. Furthermore, for positive κ_I , all the eigenvalues must also be in the left-half plane. Therefore, for any $\kappa_P, \kappa_I > 0$, by Lyapunov's indirect method, we conclude that the zero-input ($v_{ref} = 0$) error-dynamics in (21) is asymptotically stable at the equilibrium point $\delta = 0, \zeta = 0$. \square

Observe that in the context of Figure 2, the velocity reference command can be viewed as a disturbance entering the closed-loop system. It is well known that the PI control scheme is able to reject slowly varying disturbances ensuring that formation error asymptotically converges to the origin, as desired. Furthermore, from Theorem 2, it is also verified that the formation will



(a) An MIR formation tracking a leader with a PI controller.



(b) The steady-state error $\|\delta(t)\|$ asymptotically converges to 0.

Fig. 3: PI Formation control with velocity reference.

move at a constant (i.e., bounded) velocity. Thus, the PI control scheme is able to ensure zero steady-state error of the formation while tracking the velocity command of the leader.

V. SIMULATIONS

We now demonstrate the results of Theorem 4 with a numerical example. Consider a group of 6 mobile agents implementing the PI formation controller (20). A single leader is injected with a reference velocity forming a circle. The resulting trajectories are shown in Figure 3(a); the initial positions are depicted in grey and the leader is labeled by the green node. A value of $\kappa_P = 2$ and $\kappa_I = 3$ were used for the control. As shown in Figure 3(b), the PI controller leads to a zero steady-state error for the formation.

VI. CONCLUSION

In order to solve the formation tracking problem of a multi-agent system, we augmented a distance-based rigidity control law with a PI controller on the formation error. We demonstrated that the stability of the distance error dynamics can be proven using Lyapunov's indirect method, and that the centroid of the formation moves at a speed proportional to the reference velocity.

ACKNOWLEDGEMENTS

The work presented here has been supported by the Israel Science Foundation.

REFERENCES

- [1] R. Olfati-Saber and R. M. Murray, "Graph rigidity and distributed formation stabilization of multi-vehicle systems," in *the 41st IEEE Conference on Decision and Control*, vol. 3, 2002, pp. 2965–2971.
- [2] D. Zelazo, A. Franchi, H. H. Bulthoff, and P. Robuffo Giordano, "Decentralized rigidity maintenance control with range measurements for multi-robot systems," *The International Journal of Robotics Research*, vol. 34, no. 1, pp. 105–128, 01 2015.
- [3] B. Anderson, C. Yu, B. Fidan, and J. Hendrickx, "Rigid graph control architectures for autonomous formations," *IEEE Control Systems Magazine*, vol. 28, no. 6, pp. 48–63, 2008.
- [4] B. Anderson, B. Fidan, C. Yu, and D. Walle, "UAV formation control: Theory and application," in *Recent Advances in Learning and Control*. Springer, 2008, pp. 15–33.
- [5] M. A. Belabbas, "On global feedback stabilization of decentralized formation control," in *the 50th IEEE Conference on Decision and Control and European Control Conference (CDC-ECC)*, 2011, pp. 5750–5755.
- [6] D. V. Dimarogonas and K. H. Johansson, "On the stability of distance-based formation control," in *the 47th IEEE Conference on Decision and Control*, 2008, pp. 1200–1205.
- [7] T. Eren, P. N. Belhumeur, B. D. Anderson, and A. S. Morse, "A framework for maintaining formations based on rigidity," in *the 15th IFAC World Congress*, Barcelona, Spain, 2002, pp. 2752–2757.
- [8] L. Krick, M. E. Broucke, and B. A. Francis, "Stabilisation of infinitesimally rigid formations of multi-robot networks," *International Journal of Control*, vol. 82, no. 3, pp. 423–439, 2009.
- [9] L. Asimow and B. Roth, "The rigidity of graphs," *Transactions of the American Mathematical Society*, vol. 245, pp. 279–289, November 1978.
- [10] A. Y. Alfakih, "On the dual rigidity matrix," *Linear Algebra and its Applications*, vol. 428, no. 4, pp. 962–972, 2008.
- [11] L. Krick, "Application of graph rigidity in formation control of multi-robot networks," Ph.D. dissertation, University of Toronto, 2007.
- [12] F. Dörfler and B. Francis, "Formation control of autonomous robots based on cooperative behavior," in *European Control Conference*, Budapest, Hungary, 2009, pp. 2432–2437.
- [13] H. Su, X. Wang, and Z. Lin, "Flocking in multi-agent systems with a virtual leader," *IEEE Transactions on Automatic Control*, vol. 54, no. 2, pp. 293–307, 2009.
- [14] H. G. Tanner, A. Jadbabaie, and G. J. Pappas, "Flocking in fixed and switching networks," *IEEE Transactions on Automatic Control*, vol. 52, no. 5, pp. 863–868, 2007.
- [15] R. Olfati-Saber, "Flocking for multi-agent dynamic systems: Algorithms and theory," *IEEE Transactions on Automatic Control*, vol. 51, no. 3, pp. 401–420, 2006.
- [16] H. G. Tanner, A. Jadbabaie, and G. J. Pappas, "Stable flocking of mobile agents part i: Dynamic topology," in *the 42nd IEEE Conference on Decision and Control*, vol. 2, 2003, pp. 2016–2021.
- [17] O. Rozenheck, S. Zhao, and D. Zelazo, "Distance-constrained formation tracking control," in *Israel 55th Annual Conference on Aerospace Sciences*, 2015.
- [18] C. Godsil and G. Royle, *Algebraic Graph Theory*. New York: Springer, 2001.
- [19] T. Tay and W. Whiteley, "Generating Isostatic Frameworks," *Structural topology*, vol. 11, pp. 21–69, 1985.
- [20] D. V. Dimarogonas and K. H. Johansson, "Stability analysis for multi-agent systems using the incidence matrix: Quantized communication and formation control," *Automatica*, vol. 46, no. 4, pp. 695–700, April 2010.
- [21] M. Brookes, *The Matrix Reference Manual*, Imperial College, London, UK, 2005.